PLGA nanocapsules improve the delivery of Clarithromycin to kill intracellular *Staphylococcus aureus* and *Mycobacterium abscessus*

Frantiescoli Anversa Dimer [a1]†; Cristiane de Souza Carvalho-Wodarz [a1*]; Adriely Goes [a,d]; Katarina Cirnski [a,b]; Jennifer Herrmann [a,b]; Viktoria Schmitt [a, b]; Linda Pätzold[e]; Nadia Abed [c]; Chiara De Rossi [a];; Markus Bischoff [e], Patrick Couvreur [c]; Rolf Müller [a,b]; Claus-Michael Lehr [a,d*]

[a]Helmholtz Institute for Pharmaceutical Research Saarland (HIPS), Helmholtz Centre for Infection Research (HZI), Saarland University, 66123, Saarbrücken, Germany

[b]German Centre for Infection Research (DZIF), Partner Site Hannover-Braunschweig, Hannover, Germany

[c]Institut Galien Paris-Sud, UMR8612, Univ. Paris-Sud, Université Paris-Saclay, Châtenay-Malabry 92290, France

[d]Department of Pharmacy, Saarland University, 66123, Saarbrücken, Germany

[e]Institute for Medical Microbiology and Hygiene, Saarland University, Homburg, Germany.

[1]These authors contributed equally

*corresponding authors

Word Count:

Abstract: 144

Complete manuscript: 4.998

Number of references: 59

Number of figures/table: 6 figures and 1 table

CONFLICT OF INTEREST

The authors have no conflict of interest.

FINANCIAL SUPPORT

Frantiescoli A. Dimer was supported by the Brazilian *Coordenação de Aperfeiçoamento de Pessoal de Nível Superior* (CAPES) program "*Ciência sem Fronteiras*" project number BEX 18215/12-2.

ABSTRACT

Drug delivery systems are promising for targeting antibiotics directly to infected tissues. To reach intracellular *Staphylococcus aureus* and *Mycobacterium abscessus,* we encapsulated clarithromycin in PLGA nanocapsules, suitable for aerosol delivery by nebulization of an aqueous dispersion. Compared to the same dose of free clarithromycin, nanoencapsulation reduced 1,000 times the number of intracellular *S. aureus in vitro*. In RAW cells, while untreated *S. aureus* was located in acidic compartments, the treated ones were mostly situated in non-acidic compartments. Clarithromycin-nanocapsules were also effective against *M. abscessus* (70-80% killing efficacy). The activity of clarithromycin-nanocapsules against *S. aureus* was also confirmed *in vivo*, using a murine wound model as well as in zebrafish. The permeability of clarithromycin-nanocapsules across Calu-3 monolayers increased in comparison to the free drug, suggesting an improved delivery to sub-epithelial tissues. Thus, clarithromycin-nanocapsules are a promising strategy to target intracellular *S. aureus* and *M. abscessus*.

KEYWORDS

Clarithromycin; Nanoparticle; Permeability; *Staphylococcus aureus; Mycobacterium abscessus*

INTRODUCTION

Nanoparticle drug delivery systems represent a promising strategy for targeted delivery of antibiotics directly to infected tissues. In cystic fibrosis (CF) patients, infections are frequently associated with chronic inflammation and decline of lung function. The lungs of CF patients are colonized by several pathogens, including not only typical CF pathogens such as *Staphylococcus aureus* but also emerging pathogens such as *Mycobacterium abscessus* (1-3).

The association of mucus in the obstructive airway of CF patients leads to a high incidence of *S. aureus* in the lower respiratory tract (1). Besides the classical manifestations of *S. aureus* infection as a biofilm, these bacteria can survive within mammalian cells for prolonged periods (4). Inside macrophages, *S. aureus* resides within acidic phagosomes for several days, escaping afterward to the host cell cytoplasm, leading to cell death and bacterial dissemination (5-7).

M. abscessus is a fast-growing nontuberculous mycobacterium (NTM) with an increased medical and microbiological concern (8). Because of the multidrug resistance characteristic of *M. abscessus,* the treatment is a challenge, which leads to prolonged intravenous treatment, often without success (8, 9). *M. abscessus* can switch between two colony morphologies, which are strictly related to its pathogenicity: rough (R) - more virulent and persistent and smooth (S) - less virulent and biofilm-forming. The main difference between them is in the presence (S) or absence (R) of glycopeptidolipids on their surface (10).

The hydrophobic macrolide Clarithromycin (CLARI) is one of the FDA-approved antibiotics recommended in respiratory diseases due to its broad antimicrobial activity against respiratory pathogens and immunomodulatory effects (11). Long-term CLARI therapy in CF patients has been beneficial, mainly because of the down-regulation of inflammatory responses (12), which

favors patients with CF lung disease. However, CLARI treatment needs to be improved due to its limited aqueous solubility that leads to low oral bioavailability (55%), pathogen resistance, and several side effects (13, 14).

The lungs are an organ not easy to reach, and in the case of CF patients, the thick and sticky secretion produced mainly on the surface of the lower respiratory tract represents a challenge for inhaled therapies. However, inhalation nanomedicine could overcome this obstacle (15, 16). Nanocarriers based on PLGA [poly(lactic-co-glycolic acid)] are well established due to excellent biocompatibility and biodegradability of this polymer, besides being a convenient encapsulation technology and reasonable payload for a variety of drugs (15, 17). PLGA is used to prepare nanoparticles containing antibiotics with optimized release kinetics and improved efficacy compared to the free form of the drugs (15, 18-20). For instance, a pH-responsive and surface charge-switching polymeric nanoparticle delivery system with vancomycin had been described for targeting the bacterial cell wall (20). We hypothesized that nanoencapsulation of anti-infective drugs such as CLARI could ameliorate the antibiotic efficacy and overcome adverse effects such as diarrhea, nausea, vomiting, and headache, achieving better patient compliance, also after aerosol administration into the lung (21-25). Inhalable nanocarriers, like polymeric nanoparticles, are considered as an appropriate carrier to transport a drug across the extracellular and cellular barrier into the lung (26). Enhanced cellular uptake and anti-*Mycobacterium avium* intracellular activity in human blood-derived macrophages have been achieved with liposome formulations of CLARI and ofloxacin (27, 28). Other groups have also described nano- or micro-formulations with CLARI for pulmonary delivery (21-25, 29). While those nanoparticles have shown an antibacterial effect against extracellular *S. aureus* (24, 25), to the best of our

knowledge, the use of CLARI-nanoparticles to fight intracellular *S. aureus* or *M. abscessus* remained so far unexplored.

For intracellular delivery of antimicrobial agents, nanoparticle properties play a significant role. For instance, the nanoparticle surface charge is considered a key factor for the intracellular pharmacokinetics of both nanoparticles and encapsulated drug (30). Charge modification of the nanoparticle surface may, therefore, improve the interaction with mammalian or bacterial cell membranes. Once drug carriers reach the site of infection, electrostatic interactions with the negative surface of different bacterial species should be beneficial for the outcome of treatment of infectious disease, as already demonstrated using positively charged substances such as chitosan (CS) (31, 32), Eudragit®(33) or peptides (34). For example, chitosan, a natural and biodegradable polysaccharide can better attach to the bacterial cell wall and biofilms, thus adding bioadhesion and penetration enhancement as desirable pharmaceutical properties (35). Therefore, the surface charge of nanoparticles might add value to the intracellular delivery of drug-loaded nanoparticles (20, 30).

We describe here a new polymeric nanocapsule (NC) system for CLARI to be administered via aerosol nebulization to reach local pulmonary infections. NCs were prepared by using PLGA as a polymer, coated or not with chitosan, and loaded with CLARI. The following parameters of NC were addressed: biocompatibility with lung cell lines, intracellular trafficking in macrophages, activity against intracellular *S. aureus* and *M. abscessus*, activity against *S. aureus in vivo* infection models: a murine wound and zebrafish, and drug permeability through a bronchial epithelial cell line.

METHODS

Preparation of non-ionic and cationic nanocapsules

Non-ionic clarithromycin nanocapsule (CLARI-NC) were prepared using interfacial polymer deposition following solvent displacement method proposed by Fessi et al. (36). Briefly, an organic phase was prepared using PLGA (0.1 g), Lipoid S-75® (0.06 g), clarithromycin (0.01 g), medium-chain triglycerides (0.17 mL), acetone (20 mL) and ethanol (5 mL). Simultaneously, polysorbate 80 (0.08 g) was solubilized in ultra-purified water (50 mL). After complete dissolution of both phases, the organic phase was added with a speed of 1 mL/s in the aqueous phase under controlled magnetic stirring at room temperature. After homogenization, the formulation was evaporated and concentrated to 10 mL under reduced pressure to altogether remove ethanol and acetone. The cationic chitosan-coated clarithromycin nanocapsule (CS-CLARI-NC) were prepared as the non-ionic formulation, with the addition of chitosan (0.01 g) in the aqueous phase. Fluorescent nanocapsules were made with the same method changing only the fluorescently labeled-polymer. The preparation of fluorescent nanocapsules, as well as the physicochemical particle characterization, are described in the supplementary material.

TEER measurements and Drug transport

Calu-3 cells were seeded on Transwell® filters (Corning 3460, growth area 1.12 cm^2, pore size 0.4 µm), as previously described (37), and cultivated for 12 – 14 days. Before and after the drug transport experiment, the transepithelial electrical resistance (TEER) was measured using a Volt-Ohm Meter (EVOM with STX-2 chopstick electrodes, World Precision Instruments, Berlin, Germany) (37). CLARI transport study across Calu-3 was performed in the first 4h of incubation after particles/drug deposition with ALICE® system; samples of 0.1 mL were withdrawn every

30 minutes from the basolateral compartment and replaced with 0.1 mL pre-warmed medium. Additional samples were collected after 24h of the exposure. Drug quantification was performed using LC-MS/MS. The 3-(4,5- dimethylthiazol-2-yl)-2,5-diphenyltetrazolium bromide (MTT) and lactate dehydrogenase activity (LDH) assays assessed NC cellular biocompatibility (see supplementary material).

Bacterial cultivation and antimicrobial susceptibility assay

Staphylococcus aureus Newman, *Staphylococcus carnosus* DSM-20501 and *Streptococcus pneumonia* DSM-20566 were either obtained from the German Collection of Microorganisms and Cell Cultures (*Deutsche Sammlung für Mikroorganismen und Zellkulturen*, DSMZ) or were part of our internal strain collection. *M. abscessus subsp. abscessus*, rough and smooth variants, were isolated from the sputum of CF patients (38) and kindly provided by Prof. Dr. John Perry, Newcastle University. Overnight bacterial cultures conditions and susceptibilities assays are detailed described in the supplementary material.

Infection of the murine macrophage cell line and NC incubation

RAW264.7 cells were seeded in 24-well plates in RPMI with 10% fetal bovine serum (FBS) at a concentration of 2.5×10^5 cells per well and allowed to adhere overnight. The medium was removed from the wells, and the cells were washed twice with phosphate-buffered saline (PBS). An inoculum of 3×10^6 CFU of *S. aureus* or *M. abscessus* - a multiplicity of infection (MOI) = 10 - was added to each well in RPMI with 10% FBS. After 2h, infected cells with *S. aureus* were washed five times with PBS and incubated with fresh medium (RMPI with 10% FBS) containing 50 μg/mL of gentamicin for 90 min at 37°C to kill remaining extracellular bacteria. For *M.*

abscessus infection, the procedure was the same as for *S. aureus*, except that no antibiotic was used after two hours to kill extracellular bacteria since after the wash steps extracellular mycobacteria are removed. The cells were washed five additional times with PBS and then treated with Milli-Q water (CONTROL), CS-BLANK-NC, BLANK-NC, CLARI, CLARI-NC, and CS-CLARI-NC in RPMI with 10% FBS for 18h or 24h. CLARI final concentration was 10 µg/mL, either as a free or encapsulated drug. Bacterial survival was determined thought the Colony Forming Unity (CFU) (see supplementary material).

Murine S. aureus wound infection model

Animal experiments were performed with the approval of the animal welfare committee Landesamt für Verbraucherschutz (Saarbrücken, Germany) and conducted following the national guidelines for the ethical and human treatment of animals. Preparation of the bacterial inoculum and wound infection was carried out as described in the supplementary material. *S. aureus* Newman infected wounds were treated with 10 µL of CLARI-NC or BLANK-NC (sham-treated control), in a final concentration of 10 µg/mL, which were spotted onto infected wounds at 3, 48, and 96 hours post-infection. Mice were sacrificed at day 6 post-infection, full-thickness tissues harvested and homogenized in 1 ml PBS each. Serial dilutions of the homogenates were plated on sheep blood agar plates. CFU rates were determined after 24 h of growth at 37°C.

Fish lines, husbandry, embryo production and infection

Zebrafish (*Danio rerio*) embryos/larvae of the wild-type AB line were used in this study. All experiments were done with embryos/larvae at ≤ 120 hours post-fertilization (hpf), and are thus not considered as animal experiments according to the EU Directive 2010/63/EU. Protocols for husbandry and care of adult animals are in accordance with the German Animal Welfare Act

(§11 Abs. 1 TierSchG). Embryos/larvae were infected with *S. aureus* Newman and the survival determined until 90 hours post-infection (hpi). The infection procedure is described in details in the supplementary material.

Lysotracker red staining and image analysis

The samples were prepared as described for intracellular antibacterial activity assays and treated for 18h with 10 µg/mL of CLARI-NC, CS-CLARI-NC or CLARI (free drug). Lysosomes of RAW246.7 cells were stained for two h using LysoTracker Red DND-99 (200 nM). The samples preparation and imaging are described in the supplementary material.

Data Analysis

All data are expressed as mean ± SD. The results were analyzed using the GraphPad Prism 6.0c (GraphPad Software, La Jolla California USA) or Sigma Plot (Systat Software Inc., San Jose California USA). A probability (p) of less than 0.05 was considered statistically significant.

RESULTS

Clarithromycin loaded nanocapsules with non-ionic (CLARI-NC) and cationic surface (CS-CLARI-NC) were prepared using PLGA and chitosan. The particle size of either nanocarrier was in the order of 100 nm with low polydispersity indexes. Low pH (4.2) and positive zeta potential (+16.5 mV) of CS-CLARI-NC confirmed the cationic surface due to the presence of chitosan around the nanocapsules. The clarithromycin loading rate was 23.8 and 23.2 mg/g for CLARI-NC and CS-CLARI-NC, respectively (Table 1). The lower pH of chitosan-coated nanoparticles, as well as the Zeta potential, did not disturb particles stability, as shown by similar particle size

and PdI (Figure S1). For both formulations, clarithromycin release was approximately 65% after 24h (Figure S2).

To ensure the further potential use of loaded NC against respiratory infections, the biocompatibility of these formulations was assessed in bronchial and alveolar epithelial cells as well as in macrophages, in different concentration ranges (1-100 µg/mL). No apparent toxicity was observed in Calu-3 or THP-1 cells. However, A549 cells appear to be more susceptible to higher concentrations (Figure S3). To work within a safe concentration range, we used 10 µg/mL of CLARI in all further experiments, which is also in the range of clinically relevant CLARI concentrations (6 to 50µg/mL) (40).

As macrophages are the first immune cells responding to pathogens, we assessed clarithromycin nanocapsules internalization. In RAW264.7 cells, the nanocapsules were efficiently phagocytosed (Figure 1A), without affecting cell viability (Figure 1B), which was the same for the free drug, drug-loaded and drug-free ("Blank") nanocarriers. Nevertheless, the number of nanocarriers internalized per cell was significantly higher in the presence of chitosan (Figure 1C). Nanocarriers were found in lysosomes, as observed by the colocalization with LysoTracker Red fluorescence, with the chitosan-coated nanocarriers showing the most prominent lysosomal association (Figure 1D).

After demonstrating that NC loaded with CLARI localized in lysosomes, we investigated whether the encapsulation of this macrolide would have an impact on its intracellular antimicrobial activity. For *S. aureus*, the MIC of CLARI was 2X lower than those observed for either nanocarrier (Figure 2A). Similar MIC for both, free drug and nanocapsules, was however observed for *S. pneumonia* and *S. carnosus* (Table S1). Higher antimicrobial activity for both

nanocarriers was observed after the treatment of *S. aureus*-infected macrophages for 18h, where the number of intracellular *S. aureus* (indicated by the mean fluorescence) was significantly reduced compared to either the untreated or CLARI-treated RAW264.7 (Figure 2B). Intracellular bacterial survival was further investigated by using CFU counting. The results confirmed the higher efficacy of CS-CLARI-NC and CLARI-NC compared to the free CLARI after 18h treatment, with a 3-log reduction in the number of colonies compared to untreated culture. Similar results were obtained, reducing the treatment time from 18 to 2 hours, and continuing the incubation with fresh medium (Figure 2C-D).

To understand the improved anti-*S. aureus* activity of CLARI loaded NCs *in vitro,* we investigated the intracellular traffic of *S. aureus* and NCs in infected cells. CLSM revealed intracellular localization of *S. aureus* in macrophages (Figure 3A), with a significant degree of association with CS-CLARI-NC compared to CLARI-NC (Figure 3B). Once inside macrophages, *S. aureus* locates predominantly in the acidic phagosome, which favors bacterial survival (6). Our results also showed that in untreated macrophages, *S. aureus* cells survive in acidic phagosomes, as observed by the association with lysotracker red. However, the treatment with CS-CLARI-NC, CLARI–NC, or free CLARI resulted in less colocalization of *S. aureus* phagosomes to acidic compartments (Figure 3C).

We further investigated the antibacterial effect of CS-CLARI-NC against *M. abscessus*, smooth or rough variants (Figure 4). Loaded NC and free CLARI showed significant anti-mycobacterial effects either after 24h treatment (Figure 4B, E) or after 2 hours treatment followed by 22h incubation with fresh medium (Figure 4C, F). The treatment with CS-CLARI-NC for 24h reduced the colony numbers of *M. abscessus* smooth significantly, compared to the free drug (Figure 4B). As expected, CS-BLANK-NC did not have an anti-mycobacterial effect.

Because of the favorable safety profile in our Zebrafish model (data not shown), we selected only chitosan free NC (CLARI-NC) for further testing of antimicrobial activity *in vivo*, using zebrafish and murine wound infection models. After 2 hours post-infection (hpi), the larvae were either exposed to nanoparticles or the free drug. Microscopic evaluation of the infected and nanoparticle treated zebrafish revealed that nanoparticles accumulated preferentially in the yolk sack (Figure S4A) or around the eyes (Figure S4B). Larvae infected via yolk circulation valley (YCV) and treated with CLARI-NC 100 µg/mL showed a survival rate of 55% after 42 hours (Figure 5A), and a reduction in CFU of 34% after 90 hpi (Figure S4C). An even better survival rate was however observed in larvae that were infected via the fourth hindbrain ventricles (4V) and treated with CLARI-NC for 42 hours. Here, an 94% survival rate (Figure 5B), and a CFU reduction of 75% after 90 hpi was observed when compared to the infected control (Figure S4C). A comparable anti-*S. aureus* effect was observed when an *S. aureus* wound infection model was applied (Figure 5C). Topical treatment of *S. aureus* infected wounds with CLARI-NC (10 µl of a 10 µg/ml solution) at 3 h, 48 h, and 96 h post-infection significantly reduced the bacterial load within wounds at six days post-infection when compared to the NC treated control (Figure 5C).

Given that the primary use for these formulations will be aerosol deposition in the lung, we next investigated the interaction of nanocapsules with Calu-3 cells grown at the air-liquid interface (ALI). After incubation for 4 and 24h, most particles were attached to the cells rather than being internalized, and both NCs did not alter the actin cytoskeleton organization of Calu-3 (Figure 6A-D). Since the beginning of the deposition, a higher transport of CLARI through Calu-3 monolayer could be observed for both nanoparticles formulations compared to free CLARI; moreover, clarithromycin transport from CS-CLARI-NC was significantly higher to the basolateral side after 24h (Figure S5A). To confirm the consistency of permeability results, we

also assessed the transport of sodium fluorescein (NaFlu), a hydrophilic molecule typically used to evaluate paracellular permeability. There was an increased transport of NaFlu across the epithelial barrier in samples incubated with CS-CLARI-NC (Figure S5B). This suggests a moderate opening of the tight junctions, but not otherwise severe effects on epithelial barrier integrity: there were no changes observed after immunostaining for zonula occludens-1 (ZO-1), a tight junction protein (Figure S5C, D) and there was no measurable effect on epithelial barrier integrity, as indicated by practically unchanged TEER values (Figure S6).

DISCUSSION

Surface modification is a well-known approach to increase cellular uptake of polymeric nanocarriers (41). We used PLGA and chitosan, two well-established, biodegradable and biocompatible pharmaceutical polymers, which, as expected, did not induce cytotoxic effects on all cell lines we tested. Both nanocarriers showed similar parameter values regarding drug encapsulation, particle size, and controlled release of CLARI. Particles with a size of ~150 nm are considered appropriate for cellular uptake by macrophages (42).

As the primary aim was to improve the delivery of clarithromycin to bacteria localized inside alveolar macrophages during infections, we used the well-characterized RAW mouse macrophage cell line as a model to study particle uptake and intracellular localization. We analyzed confocal images of RAW264.7 cells containing NC and quantified with ImageJ, in which co-localization experiments identified the NC intracellular location. Chitosan-coated particles were taken up better than particles without chitosan, proving that the cationic surface may improve the intracellular uptake. The former particles also showed stronger accumulation in lysosomes as observed by LysoTracker red – a cationic fluorescent dye that accumulates in acidic compartments as an indicator of lysosomal content, a behavior also described by others

(43). While the lysosomal degradation of PLGA nanocarriers remains to be investigated in more detail, the co-localization with lysosomes is at least likely to enhance drug release and polymer degradation (30), also contributing to the safe elimination of such nanocarriers. The long-term fate of such particles remains to be further elucidated in more detail. Cellular stress generated upon exposure to most NPs can activate autophagy (41), the intracellular mechanism responsible for degrading undesirable substances (44-46). Further studies shall address to what extent autophagy plays a role in the cellular elimination of both nanocapsules.

The intracellular bioavailability of an antibiotic depends on the penetration into the host cell, the accumulation inside the cell, and the cellular metabolism (15). As *S. aureus* can infect macrophages, we evaluated the bactericidal effect of internalized nanocapsules against intracellular *S. aureus*. For *S. aureus,* the MIC of free CLARI was 2X lower than the one observed for encapsulated CLARI. These results indicate that there is a controlled release of CLARI once encapsulated in PLGA NC, what is expected, and the encapsulation did not hamper the activity of this antibiotic against extracellular *S. aureus*. As also expected, CS-BLANK-NC did not show any antibacterial activity. However, the *in vitro* efficacy of CLARI to kill intracellular bacteria was significantly improved by drug encapsulation into a polymeric nanocarrier.

To acknowledge the limited pulmonary residence time of an inhaled antibiotic, we treated the infected cells for 2h, washed the cultures and replaced with fresh medium without drug or formulations, for further 18h. Under such conditions, the two nanocarriers were still more effective in killing the intracellular *S. aureus* compared to the free drug. There was even a slight, but significant better activity of the CS-CLARI-NC, suggesting that the positive zeta potential

conveyed by this natural cationic polymer further improves the intracellular delivery of such antibiotic nanocarriers.

Once internalized in macrophages, *S. aureus* avoids its lysosomal digestion, and escape into the host cell cytoplasm, eventually inducing host cell death (47). The latter leads to the release of bacteria into the extracellular space, where they proliferate and invade new cells. A recent publication showed that methicillin-resistant *S. aureus* (MRSA) of the USA300 lineage traffic to mature phagolysosomes in murine RAW macrophages, without disrupting normal phagosome acidification (6). Conversely *S. aureus* blocks phagolysosomal maturation leading to bacterial persistence in macrophages (48). In our study with *S. aureus* strain Newman, we also observed that the bacterial cells were located in acidic compartments and that the treatment with formulations as well as free CLARI decreased the colocalization of *S. aureus* with acidic compartments. Whether this effect is due to an inhibition of phagosomal acidification or the escape of *S. aureus* from acidic vacuoles to the cell cytoplasm are still open questions.

The traffic of chitosan nanoparticles to phagosomes might help in fighting bacteria living in such acidic compartments (30). As the nanoparticles were mostly concentrated in lysosomes, the release of CLARI into an acidic compartment would favor the killing of *S. aureus* in an acidic phagosome. Our results also suggest that CLARI-NCs disrupt the *S. aureus* intra-macrophage survival and thereby the regular cycle of infected macrophage lysis. The properties of phagosomes results from a complex series of interaction with the endolysosomal and several pathogens disrupt such maturation to survive (49). As far as our studies went, we cannot unequivocally prove that NC and *S. aureus* were co-localized in late phagolysosome or lysosomes. As previously reported *S. aureus* resides in early-stage phagosomes while the NC is more like to end up in the late phagolysosome (48, 50). As published by the Griffiths and co-

workers (50), PLGA nanoparticles containing rifampicin and coumarin-6 were located in the phagolysosome of macrophages and separated from intracellular *Mycobacterium bovis* BCG. Nevertheless, sufficient antibiotic was released into the infected cell cytoplasm to clear the infection in a mouse *in vivo* model of mycobacterial infection (50). There is evidence that CLARI also works as a potent inhibitor of autophagy and lysosomal function (40). Whether this aspect of CLARI accounts for the *S. aureu*s killing mechanism in the present study remains to be investigated.

M. abscessus is a nontuberculous mycobacterium responsible for lung diseases and healthcare-associated extrapulmonary infections. The resistance to antibiotics is the main issue in the treatment of infections caused by this mycobacterium (51). Nanomedicine has been considered a potential strategy to overcome mycobacterial resistance, as explored by some groups. Of note, a liposomal formulation containing amikacin was developed and showed good improvement in killing *M. abscessus* and *M. avium*, both *in vitro* and *in vivo* (52), but they have not been tested against both smooth and rough variant of the mycobacteria. Moreover, to the best of our knowledge, this is the first time that a nanomedicine of CLARI was used against *M. abscessus*.

Nevertheless, macrolide resistance in *M. abscessus* has been widely reported, which suggest that the use of CLARI must be carefully evaluated. Inducible resistance to CLARI occurs when the strain is susceptible to this macrolide after three days of treatment, but becomes resistant after 14 days, with a MIC $\geq$ 8 μg/mL (53). The clinical strains used in our work were not resistant to CLARI since the MIC after 14 days was around 4 μg/mL (data not shown); others also described similar MICs for *Mycobacterium avium*-intracellulare (27). Particle treatment was efficient to kill both smooth and rough forms of *M. abscessus*, as it was also observed for the free drug. For aerosolized therapy, CLARI must be solubilized in DMSO due to its poor solubility in water,

which is of course not easily translatable to the clinic. However, this solvent allows for the complete availability of the free CLARI creating in this way a relevant control for our drug-loaded nanocarriers regarding drug efficacy assessment *in vitro*. Regarding a potential administration to patients, it is essential to point out that CLARI-loaded nanocarriers can be easily dispersed in water and subsequently aerosolized.

To demonstrate the *in vivo* efficacy of our drug-loaded nanocarriers, two different *S. aureus* infection models were used: zebrafish and a murine wound. Treatment of infected animals with CLARI-NC significantly reduced the bacterial loads in both models. However, the highest survival rates were observed in the CLARI-NC 100 µg/mL group, suggesting that the drug-loaded NCs are superior over the free drug in protecting the vertebrates against *S. aureus* in the zebrafish model. For the murine model, the bacterial reduction could be seen already with NC-CLARI 10 µg/mL. Topical application of CLARI-NC with the lower dose still reduced the bacterial load in the infected wounds by more than 99%, demonstrating that CLARI-NC are active in a mammalian model.

Despite the significant decrease in the number of viable bacteria (either *S. aureus* or *M. abscessus*) after the treatment with both NC *in vitro*, not all the intracellular bacteria were eradicated at the time frame of incubation used in this work, which might represent a problem since the remaining bacteria can multiply again. The same was observed in our *in vivo* experiments. Further studies with long terms treatment and repeated doses of application would be necessary to guarantee complete bacteria elimination.

Besides the antimicrobial effect, macrolides have several beneficial effects on inflammation and cellular damage. In the airway, they increase the mucociliary clearance and the tight junctions

functionality (54). After deposition of aerosolized CLARI-loaded nanocarriers at the ALI of Calu-3 cells, we observed a moderate enhancement of transepithelial transport but no drastic disruption of epithelial barrier function. Most of the particles were only attached to the surface of Calu-3 cells rather than internalized, which might account for their good biocompatibility. Our transport results agree with previous work from Zakeri-Milani and colleagues, which had reported a higher permeation of CLARI when nanoencapsulated (55). The increased transport of CS-CLARI-NC may be assigned to a reversible opening of the tight junctions caused by an electrical interaction between the positive charge of the nanocapsules and the negative charge of the cell membranes as previously reported (56, 57). Therefore, the positive charge represented by the positive zeta potential and arisen by chitosan presence increased the NC adsorption to the cell surface (composed mainly of phospholipids) (58, 59).

In conclusion, we demonstrated that nanocapsules loaded with CLARI were significantly more effective in killing intracellular *S. aureus*, as well as both variants of *M. abscessus,* than the same dose of the same drug in free form. Nanomedicines might thus add considerable value to the combat against infectious diseases, especially in the context of polymicrobial infections as well as bacterial multi-resistance in CF patients.

APPENDIX A. SUPPLEMENTARY DATA

The following is the supplementary data to this article.

AUTHOR INFORMATION

Corresponding Authors

*Helmholtz Institute for Pharmaceutical Research Saarland (HIPS), University Campus E8 1, Saarland University, 66123, Saarbrücken, Germany. Tel.: +49 681 98806 1002; fax: + 49 681 98806 1009.

E-mail addresses:

cristiane.carvalho@helmholtz-hzi.de;

Claus-Michael.Lehr@helmholtz-hips.de

Present Addresses

† Inovat – Grupo União Química, 07112-070, Guarulhos, Brazil.

ACKNOWLEDGMENTS

We thank Prof. Dr. John Perry for the mycobacterial strains, Mr. Maik Wodarz for helping with the ImageJ plugin writing, Mrs. Jana Westhues for helping with RAW264.7 cell cultivation, Mr. Pascal Paul for helping with nanoparticles preparation and nanoparticles stability assay, and Dr. Maximiliano G. Gutierrez for the critical reading.

REFERENCES

1. Ulrich M, Herbert S, Berger J, Bellon G, Louis D, Münker G, et al. Localization of Staphylococcus aureus in Infected Airways of Patients with Cystic Fibrosis and in a Cell Culture Model of S. aureus Adherence. American Journal of Respiratory Cell and Molecular Biology. 1998;19(1):83-91.

2. Bauernfeind A, Hörl G, Jungwirth R, Petermüller C, Przyklenk B, Weisslein-Pfister C, et al. Qualitative and quantitative microbiological analysis of sputa of 102 patients with cystic fibrosis. Infection. 1987;15(4):270-7.

3. Filkins LM, O'Toole GA. Cystic Fibrosis Lung Infections: Polymicrobial, Complex, and Hard to Treat. PLoS Pathog. 2015;11(12):e1005258.

4. Garzoni C, Kelley WL. Staphylococcus aureus: new evidence for intracellular persistence. Trends in Microbiology.17(2):59-65.

5. Tranchemontagne ZR, Camire RB, O'Donnell VJ, Baugh J, Burkholder KM. Staphylococcus aureus Strain USA300 Perturbs Acquisition of Lysosomal Enzymes and Requires Phagosomal Acidification for Survival inside Macrophages. Infect Immun. 2015;84(1):241-53.

6. Flannagan RS, Heit B, Heinrichs DE. Intracellular replication of Staphylococcus aureus in mature phagolysosomes in macrophages precedes host cell death, and bacterial escape and dissemination. Cell Microbiol. 2016;18(4):514-35.

7. Lopez de Armentia MM, Amaya C, Colombo MI. Rab GTPases and the Autophagy Pathway: Bacterial Targets for a Suitable Biogenesis and Trafficking of Their Own Vacuoles. Cells. 2016;5(1).

8. Mougari F, Guglielmetti L, Raskine L, Sermet-Gaudelus I, Veziris N, Cambau E. Infections caused by Mycobacterium abscessus: epidemiology, diagnostic tools and treatment. Expert Rev Anti Infect Ther. 2016;14(12):1139-54.

9. Novosad SA, Beekmann SE, Polgreen PM, Mackey K, Winthrop KL, Team MaS. Treatment of Mycobacterium abscessus Infection. Emerg Infect Dis. 2016;22(3):511-4.

10. Byrd TF, Lyons CR. Preliminary characterization of a Mycobacterium abscessus mutant in human and murine models of infection. Infect Immun. 1999;67(9):4700-7.

11. Zuckerman JM, Qamar F, Bono BR. Review of Macrolides (Azithromycin, Clarithromycin), Ketolids (Telithromycin) and Glycylcyclines (Tigecycline). Medical Clinics of North America. 2011;95(4):761-91.

12. Pukhalsky AL, Shmarina GV, Kapranov NI, Kokarovtseva SN, Pukhalskaya D, Kashirskaja NJ. Anti-inflammatory and immunomodulating effects of clarithromycin in patients with cystic fibrosis lung disease. Mediators Inflamm. 2004;13(2):111-7.

13. Bermudez LE, Nash K, Petrofsky M, Young LS, Inderlied CB. Clarithromycin-Resistant Mycobacterium avium Is Still Susceptible to Treatment with Clarithromycin and Is Virulent in Mice. Antimicrobial Agents and Chemotherapy. 2000;44(10):2619-22.

14. Global Alliance for TB Drug Development. Clarithromycin. Tuberculosis. 2008;88(2):92-5.

15. Xiong MH, Bao Y, Yang XZ, Zhu YH, Wang J. Delivery of antibiotics with polymeric particles. Adv Drug Deliv Rev. 2014;78(0):63-76.

16. Henning A, Hein S, Schneider M, Bur M, Lehr CM. Pulmonary drug delivery: medicines for inhalation. Handb Exp Pharmacol. 2010(197):171-92.

17. Danhier F, Ansorena E, Silva JM, Coco R, Le Breton A, Préat V. PLGA-based nanoparticles: An overview of biomedical applications. Journal of Controlled Release. 2012;161(2):505-22.

18. Cheow W, Chang M, Hadinoto K. Antibacterial Efficacy of Inhalable Levofloxacin-Loaded Polymeric Nanoparticles Against E. coli Biofilm Cells: The Effect of Antibiotic Release Profile. Pharmaceutical Research. 2010;27(8):1597-609.

19. Misra R, Acharya S, Dilnawaz F, Sahoo SK. Sustained antibacterial activity of doxycycline-loaded poly(D,L-lactide-co-glycolide) and poly(epsilon-caprolactone) nanoparticles. Nanomedicine (Lond). 2009;4(5):519-30.

20. Radovic-Moreno AF, Lu TK, Puscasu VA, Yoon CJ, Langer R, Farokhzad OC. Surface Charge-Switching Polymeric Nanoparticles for Bacterial Cell Wall-Targeted Delivery of Antibiotics. ACS Nano. 2012;6(5):4279-87.

21. Moghaddam PH, Ramezani V, Esfandi E, Vatanara A, Nabi-Meibodi M, Darabi M, et al. Development of a nano–micro carrier system for sustained pulmonary delivery of clarithromycin. Powder Technology. 2013;239(0):478-83.

22. Park C-W, Li X, Vogt FG, Hayes Jr D, Zwischenberger JB, Park E-S, et al. Advanced spray-dried design, physicochemical characterization, and aerosol dispersion performance of vancomycin and clarithromycin multifunctional controlled release particles for targeted respiratory delivery as dry powder inhalation aerosols. International Journal of Pharmaceutics. 2013;455(1–2):374-92.

23. Pilcer G, Rosiere R, Traina K, Sebti T, Vanderbist F, Amighi K. New co-spray-dried tobramycin nanoparticles-clarithromycin inhaled powder systems for lung infection therapy in cystic fibrosis patients. J Pharm Sci. 2013;102(6):1836-46.

24. Mohammadi G, Nokhodchi A, Barzegar-Jalali M, Lotfipour F, Adibkia K, Ehyaei N, et al. Physicochemical and anti-bacterial performance characterization of clarithromycin nanoparticles as colloidal drug delivery system. Colloids and Surfaces, B: Biointerfaces. 2011;88(1):39-44.

25. Valizadeh H, Mohammadi G, Ehyaei R, Milani M, Azhdarzadeh M, Zakeri-Milani P, et al. Antibacterial activity of clarithromycin loaded PLGA nanoparticles. Pharmazie. 2012;67(1):63-8.

26. d'Angelo I, Conte C, Miro A, Quaglia F, Ungaro F. Pulmonary drug delivery: a role for polymeric nanoparticles? Curr Top Med Chem. 2015;15(4):386-400.

27. Onyeji CO, Nightingale CH, Nicolau DP, Quintiliani R. Efficacies of liposome-encapsulated clarithromycin and ofloxacin against Mycobacterium avium-M. intracellulare complex in human macrophages. Antimicrob Agents Chemother. 1994;38(3):523-7.

28. Salem, II, Duzgunes N. Efficacies of cyclodextrin-complexed and liposome-encapsulated clarithromycin against Mycobacterium avium complex infection in human macrophages. Int J Pharm. 2003;250(2):403-14.

29. Manniello MD, Del Gaudio P, Porta A, Aquino RP, Russo P. Aerodynamic properties, solubility and in vitro antibacterial efficacy of dry powders prepared by spray drying: Clarithromycin versus its hydrochloride salt. Eur J Pharm Biopharm. 2016;104:1-6.

30. Xie S, Tao Y, Pan Y, Qu W, Cheng G, Huang L, et al. Biodegradable nanoparticles for intracellular delivery of antimicrobial agents. Journal of Controlled Release. 2014;187(0):101-17.

31. Jeon SJ, Oh M, Yeo W-S, Galvão KN, Jeong KC. Underlying Mechanism of Antimicrobial Activity of Chitosan Microparticles and Implications for the Treatment of Infectious Diseases. PLoS ONE. 2014;9(3):e92723.

32. Kong M, Chen XG, Xing K, Park HJ. Antimicrobial properties of chitosan and mode of action: A state of the art review. International Journal of Food Microbiology. 2010;144(1):51-63.

33. Dillen K, Bridts C, Van der Veken P, Cos P, Vandervoort J, Augustyns K, et al. Adhesion of PLGA or Eudragit®/PLGA nanoparticles to Staphylococcus and Pseudomonas. International Journal of Pharmaceutics. 2008;349(1–2):234-40.

34. Wenzel M, Chiriac AI, Otto A, Zweytick D, May C, Schumacher C, et al. Small cationic antimicrobial peptides delocalize peripheral membrane proteins. Proceedings of the National Academy of Sciences. 2014;111(14):E1409-E18.

35. Lepeltier E, Loretz B, Desmaële D, Zapp J, Herrmann J, Couvreur P, et al. Squalenoylation of Chitosan: A Platform for Drug Delivery? Biomacromolecules. 2015.

36. Fessi H, Puisieux F, Devissaguet JP, Ammoury N, Benita S. Nanocapsule formation by interfacial polymer deposition following solvent displacement. International Journal of Pharmaceutics. 1989;55(1):R1-R4.

37. Dimer F, de Souza Carvalho-Wodarz C, Haupenthal J, Hartmann R, Lehr C-M. Inhalable Clarithromycin Microparticles for Treatment of Respiratory Infections. Pharmaceutical Research. 2015:1-12.

38. Preece CL, Perry A, Gray B, Kenna DT, Jones AL, Cummings SP, et al. A novel culture medium for isolation of rapidly-growing mycobacteria from the sputum of patients with cystic fibrosis. J Cyst Fibros. 2016;15(2):186-91.

39. Ribeiro GM, Matsumoto CK, Real F, Teixeira D, Duarte RS, Mortara RA, et al. Increased survival and proliferation of the epidemic strain Mycobacterium abscessus subsp. massiliense CRM0019 in alveolar epithelial cells. BMC Microbiol. 2017;17(1):195.

40. Nakamura M, Kikukawa Y, Takeya M, Mitsuya H, Hata H. Clarithromycin attenuates autophagy in myeloma cells. Int J Oncol. 2010;37(4):815-20.

41. Frohlich E. The role of surface charge in cellular uptake and cytotoxicity of medical nanoparticles. Int J Nanomedicine. 2012;7:5577-91.

42. He C, Hu Y, Yin L, Tang C, Yin C. Effects of particle size and surface charge on cellular uptake and biodistribution of polymeric nanoparticles. Biomaterials. 2010;31(13):3657-66.

43. Zubareva AA, Shcherbinina TS, Varlamov VP, Svirshchevskaya EV. Intracellular sorting of differently charged chitosan derivatives and chitosan-based nanoparticles. Nanoscale. 2015;7(17):7942-52.

44. Hulea L, Markovic Z, Topisirovic I, Simmet T, Trajkovic V. Biomedical Potential of mTOR Modulation by Nanoparticles. Trends Biotechnol. 2016;34(5):349-53.

45. Wang J, Yu Y, Lu K, Yang M, Li Y, Zhou X, et al. Silica nanoparticles induce autophagy dysfunction via lysosomal impairment and inhibition of autophagosome degradation in hepatocytes. Int J Nanomedicine. 2017;12:809-25.

46. Marquardt C, Fritsch-Decker S, Al-Rawi M, Diabate S, Weiss C. Autophagy induced by silica nanoparticles protects RAW264.7 macrophages from cell death. Toxicology. 2017;379:40-7.

47. Schroder A, Kland R, Peschel A, von Eiff C, Aepfelbacher M. Live cell imaging of phagosome maturation in Staphylococcus aureus infected human endothelial cells: small colony

variants are able to survive in lysosomes. Medical microbiology and immunology. 2006;195(4):185-94.

48. Jubrail J, Morris P, Bewley MA, Stoneham S, Johnston SA, Foster SJ, et al. Inability to sustain intraphagolysosomal killing of Staphylococcus aureus predisposes to bacterial persistence in macrophages. Cell Microbiol. 2015.

49. Flannagan RS, Cosio G, Grinstein S. Antimicrobial mechanisms of phagocytes and bacterial evasion strategies. Nat Rev Microbiol. 2009;7(5):355-66.

50. Kalluru R, Fenaroli F, Westmoreland D, Ulanova L, Maleki A, Roos N, et al. Poly(lactide-co-glycolide)-rifampicin nanoparticles efficiently clear Mycobacterium bovis BCG infection in macrophages and remain membrane-bound in phago-lysosomes. Journal of Cell Science. 2013;126(14):3043-54.

51. Nessar R, Cambau E, Reyrat JM, Murray A, Gicquel B. Mycobacterium abscessus: a new antibiotic nightmare. J Antimicrob Chemother. 2012;67(4):810-8.

52. Rose SJ, Neville ME, Gupta R, Bermudez LE. Delivery of aerosolized liposomal amikacin as a novel approach for the treatment of nontuberculous mycobacteria in an experimental model of pulmonary infection. PLoS One. 2014;9(9):e108703.

53. CLSI. Susceptibility Testing of Mycobacteria, Nocardiae, and Other Aerobic Actinomycetes; Approved Standard—Second Edition. CLSI document M24-A2 Wayne, PA: Clinical and Laboratory Standards Institute. 2011.

54. Altenburg J, de Graaff CS, van der Werf TS, Boersma WG. Immunomodulatory effects of macrolide antibiotics - part 1: biological mechanisms. Respiration. 2011;81(1):67-74.

55. Zakeri-Milani P, Islambulchilar Z, Majidpour F, Jannatabadi E, Lotfipour F, Valizadeh H. A study on enhanced intestinal permeability of clarithromycin nanoparticles. Brazilian Journal of Pharmaceutical Sciences. 2014;50(1):121-9.

56. Yang R, Yang S-G, Shim W-S, Cui F, Cheng G, Kim I-W, et al. Lung-specific delivery of paclitaxel by chitosan-modified PLGA nanoparticles via transient formation of microaggregates. Journal of Pharmaceutical Sciences. 2009;98(3):970-84.

57. Vllasaliu D, Exposito-Harris R, Heras A, Casettari L, Garnett M, Illum L, et al. Tight junction modulation by chitosan nanoparticles: Comparison with chitosan solution. International Journal of Pharmaceutics. 2010;400(1–2):183-93.

58. Pavinatto FJ, Pavinatto A, Caseli L, dos Santos DS, Nobre TM, Zaniquelli MED, et al. Interaction of Chitosan with Cell Membrane Models at the Air−Water Interface. Biomacromolecules. 2007;8(5):1633-40.

59. Mu Q, Jiang G, Chen L, Zhou H, Fourches D, Tropsha A, et al. Chemical Basis of Interactions Between Engineered Nanoparticles and Biological Systems. Chemical Reviews. 2014;114(15):7740-81.

FIGURE LEGENDS

Table 1. Nanocapsule characterization. Average particle size and polydispersity index (PdI) determined by dynamic light scattering, zeta potential by electrophoretic mobility, pH by potentiometry and drug content, and encapsulation efficiency by LC/MS-MS.

Figure 1. Nanocapsule internalization in RAW264.7 cells after 18h incubation. A) Representative Z-stack image of RAW264.7 cells containing fluorescent CS-CLARI-NCs; B) MTT assay of RAW264.7 cells incubated with free drug or NCs; C) Intracellular NCs quantification in RAW264.7 cells measured by green fluorescence per cell; D) Quantification of lysotracker red association with NCs; representative confocal pictures showing lysosome (red), nanoparticle (green) and channels overlay. n= DAPI-stained cell nucleus. Scale bar 10μm. At least 200 cells were counted per condition. *** $p< 0.0001$, 1-way ANOVA with Bonferroni post-hoc test. Error bars represent mean ± SD of 3 independent experiments (C-D).

Figure 2. **CLARI-loaded NCs activity against *S. aureus*.** A) MIC of CLARI, CS-BLANK-NC, CLARI-NC and CS-CLARI-NC against *S. aureus* in broth*;* B) Quantification of *S. aureus* detected with anti-*S.aur*eus antibody in infected RAW264.7 cells after 18h treatment; C-D) CFU of *S. aureus* at 18h hours after treatment (C) or 2 h treatment followed by 18 h incubation with fresh medium (without drug or formulations)(D). Error bar represents mean ± SD of 3 independent experiments. (** $p < 0.01$, n=3 independent experiments).

Figure 3. *S. aureus*-containing phagosome association with nanocapsules and with acidic compartments. A) Representative image of RAW264.7 cells infected with *S. aureus* Newman and treated with NCs for 18 h. Bacteria were stained with anti-*S. aureus* antibody (blue), the

acidic compartments stained with Lysotracker (red) and nanocapsules with FITC (green). Examples of no association (a1) or association (a2) of S. aureus with lysosomes or NCs are shown. Scale bar: 50 µm. B) Quantification of the association of NCs with *S. aureus* after 18 h. C) Quantification of lysotracker red association with intracellular *S. aureus* in untreated cultures and treated with NCs or free drug. Error bars represent mean ± SD from at least 200 cells from 3 independent experiments.

Figure 4. Replication of *M. abscessus* in RAW264.7 cells is restricted by NCs incubation. Representative images of *M. abscessus* smooth (A) or rough (D) morphology on 7H11 agar plate. B and E) RAW264.7 cells infected for 2 hours and treated for 24h with free drug or nanocapsules. C and F) RAW264.7 cells infected for 2h, treated for further 2h then washed and incubated with fresh medium without CLARI or formulations for 22h. Error bars represent mean ± SD from 3 independent experiments. *$p < 0.05$; ** $p < 0.001$; ***$p < 0.0001$. One-way ANOVA with Bonferroni post-hoc test.

Figure 5. Zebrafish and Murine wound infection models. A-B) Zebrafish survival is shown with Kaplan-Meier survival curves for a high-dose of *S. aureus Newman* (SaN) injection in (A) YCV and (B) 4V. Infected larvae were subsequently treated with 100 µg/mL of CLARI or CLARI-NC. Negative control: heat-inactivated SaN. Per group, 20-30 infected larvae were analyzed. C) Effect of CLARI-NC (10 µg/mL) on the bacterial loads in *S. aureus* infected murine wounds at day 6 post-infection. Negative control: BLANK-NCs (sham-treated). Each symbol represents an individual wound; horizontal bars: median of all observations (n=12). ***$p < 0.0001$ (Mann–Whitney U-test).

Figure 6. Nanocapsules association with bronchial cells. Clarithromycin nanocapsules (CLARI-NC; A, B; green) or chitosan-coated clarithromycin nanocapsules (CS-CLARI-NC; C, D; green) were deposited as an aerosol on Calu-3 cells at the air-liquid interface. Cells were fixed either at 4h (A, C) or 24h (B, D), after deposition and immunostained with rhodamine-phalloidin for actin (red) and DAPI for the nuclei. Scale bar: 20 µm.

Figures

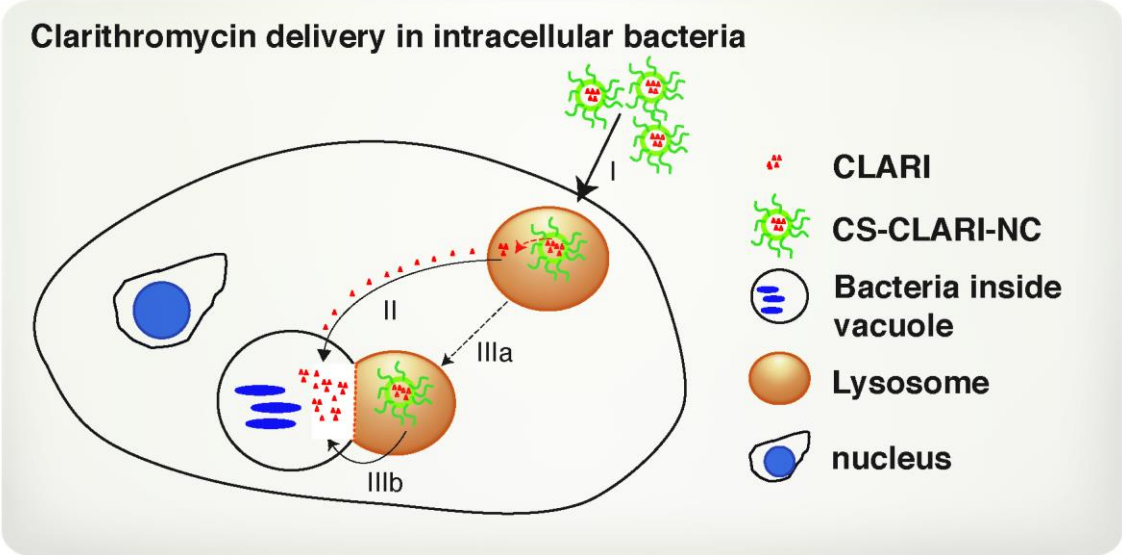

Graphic abstract

Clarithromycin delivery to intracellular bacteria in macrophages
I - Macrophage internalize CS-CLARI-NC that end-ups in lysosomes.
II - CLARI can be released in the macrophage cytoplasm and might reach the bacteria inside the vacuole.
IIIa - Lysosomes containing CS-CLARI-NC can get closer to the bacteria vacuole.
IIIb - CS-CLARI-NC and bacteria compartments are closely associate and CLARI might be released inside the bacteria vacuole.

Table 1.

	CLARI-NC	CS-CLARI-NC
Particle Size (nm)	94.9 ± 1.3	120.6 ± 2.1
PdI	0.21 ± 0.02	0.15 ± 0.01
Zeta Potential (mV)	- 28.2 ± 0.7	+ 16.5 ± 0.7
pH	5.9 ± 0.4	4.2 ± 0.2
Loading Rate (mg/g)	23.8	23.2
Drug Content (mg/mL)*	0.99 ± 0.02	0.98 ± 0.02
Encapsulation Efficiency (%)	68 ± 1.1	67 ± 0.8

* NC suspension

Figure 1.

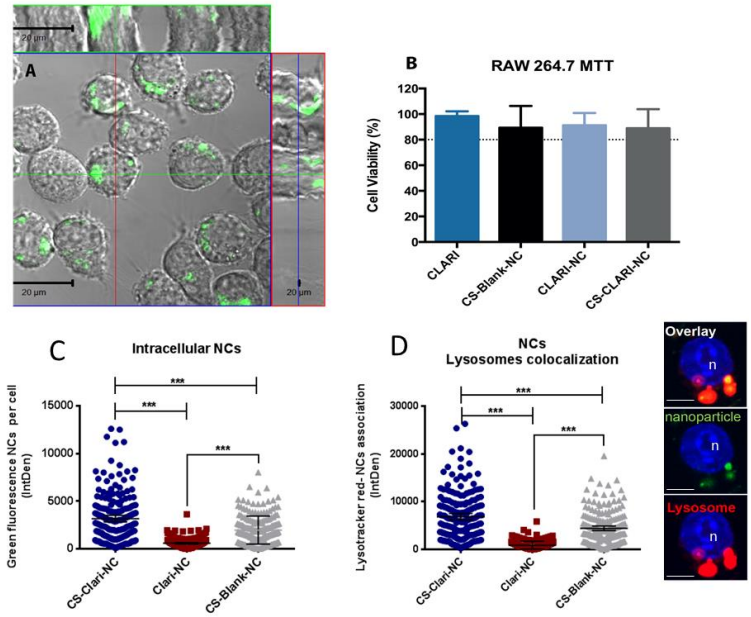

Figure 2.

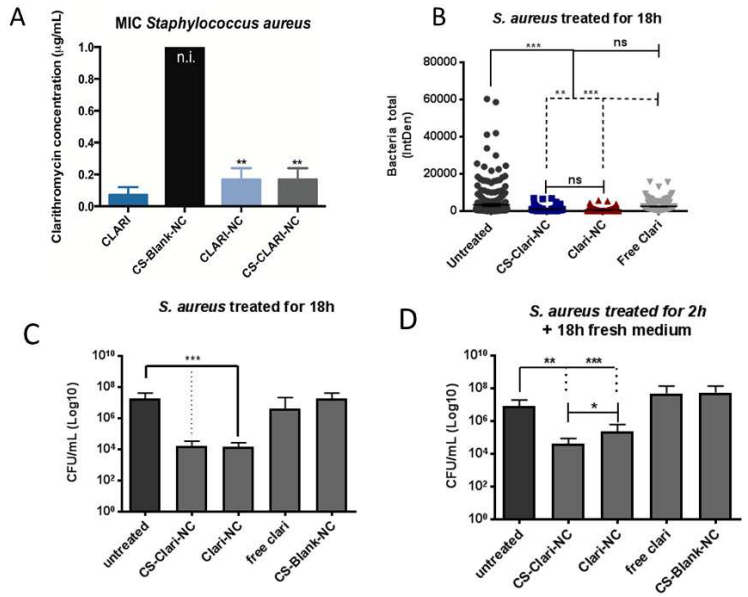

Figure 3

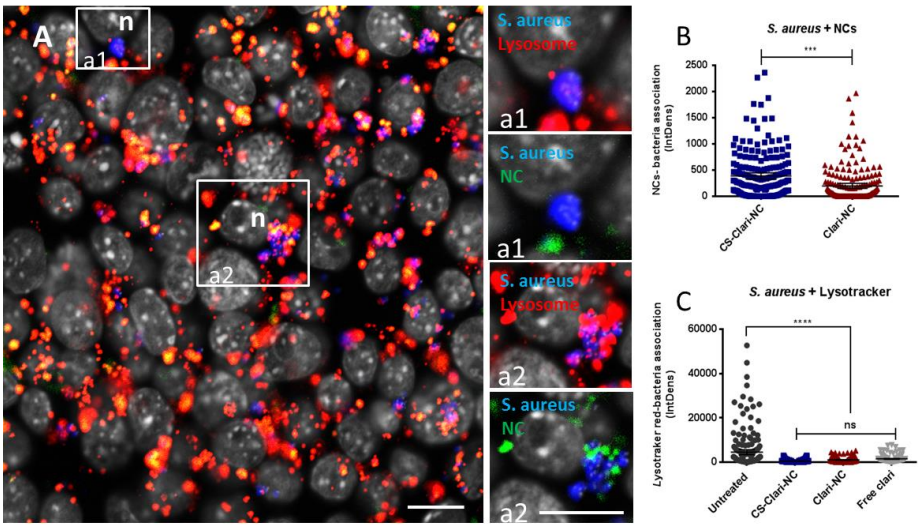

Figure 4.

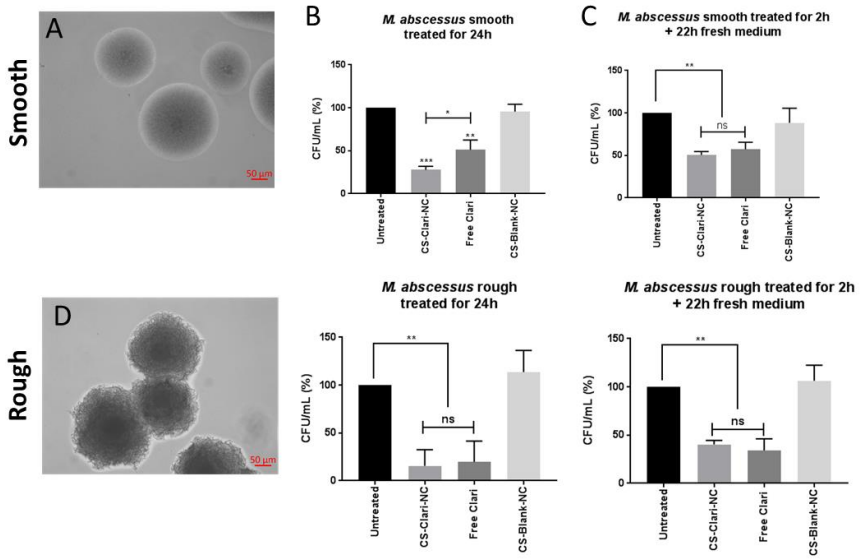

Figure 5.

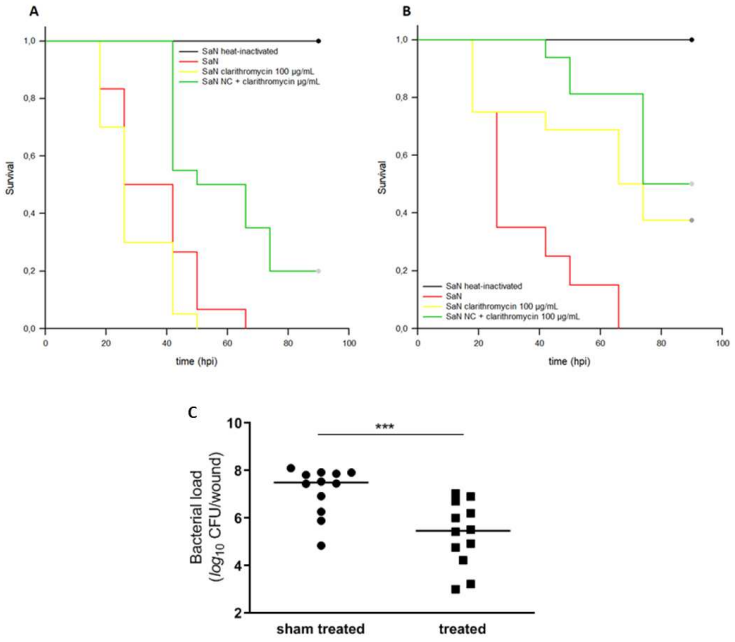

Figure 6.

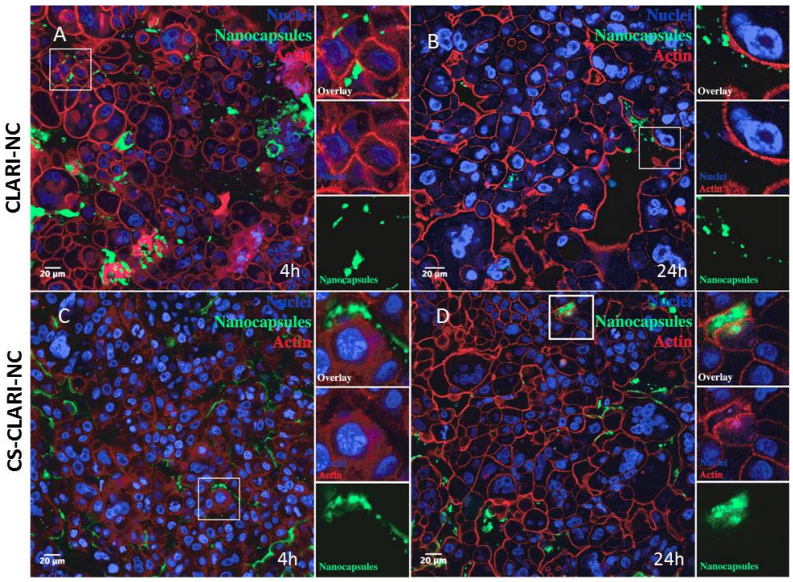
CLARI-NC
CS-CLARI-NC
A
B
C
D
Nuclei
Nanocapsules
Actin
Overlay
4h
24h
20 µm